

 Open access • Posted Content • DOI:10.1101/2021.09.02.458740

## **Distinct neutralizing kinetics and magnitudes elicited by different SARS-CoV-2 variant spikes** — [Source link](#)

Yang Liu, Jianying Liu, Jing Zou, Ping Ren ...+3 more authors

**Institutions:** University of Texas Medical Branch

**Published on:** 02 Sep 2021 - bioRxiv (Cold Spring Harbor Laboratory)

**Topics:** Neutralizing antibody and Heterologous

Related papers:

- [Comparison of Neutralizing Antibody Titers Elicited by mRNA and Adenoviral Vector Vaccine against SARS-CoV-2 Variants](#)
- [A methyltransferase-defective VSV-based SARS-CoV-2 vaccine candidate provides complete protection against SARS-CoV-2 infection in hamsters.](#)
- [A bivalent recombinant vaccine targeting the S1 protein induces neutralizing antibodies against both SARS-CoV-2 variants and wild-type of the virus.](#)
- [Protection of human ACE2 transgenic Syrian hamsters from SARS CoV-2 variants by human polyclonal IgG from hyper-immunized transchromosomal bovines](#)
- [Enhanced protective immunity against SARS-CoV-2 elicited by a VSV vector expressing a chimeric spike protein.](#)

Share this paper:    

View more about this paper here: <https://typeset.io/papers/distinct-neutralizing-kinetics-and-magnitudes-elicited-by-1xrccgol6c>

1 **Distinct neutralizing kinetics and magnitudes elicited by different SARS-CoV-2 variant**  
2 **spikes**

3 Yang Liu<sup>1,\*</sup>, Jianying Liu<sup>2,\*</sup>, Jing Zou<sup>1,\*</sup>, Ping Ren<sup>3</sup>, Scott C. Weaver<sup>2,4,5</sup>, Xuping Xie<sup>1,#</sup>, Pei-Yong  
4 Shi<sup>1,4,5,6,7,#</sup>

5 <sup>1</sup>Department of Biochemistry and Molecular Biology, University of Texas Medical Branch,  
6 Galveston TX, U.S.A.

7 <sup>2</sup>Department of Microbiology and Immunology, University of Texas Medical Branch, Galveston  
8 TX, U.S.A.

9 <sup>3</sup>Department of Pathology, University of Texas Medical Branch, Galveston, TX, U.S.A.

10 <sup>4</sup>Institute for Human Infection and Immunity, University of Texas Medical Branch, Galveston, TX,  
11 U.S.A.

12 <sup>5</sup>Sealy Center for Structural Biology & Molecular Biophysics, University of Texas Medical Branch,  
13 Galveston, TX, U.S.A.

14 <sup>6</sup>Institute for Translational Sciences, University of Texas Medical Branch, Galveston, TX, U.S.A.

15 <sup>7</sup>Sealy Institute for Vaccine Sciences, University of Texas Medical Branch, Galveston, TX, U.S.A.

16  
17 \* These authors contributed equally to this work.

18 #Correspondence: X.X. ([xuxie@UTMB.edu](mailto:xuxie@UTMB.edu)) or P.-Y.S. ([peshi@UTMB.edu](mailto:peshi@UTMB.edu))  
19

20 **Abstract**

21 The rapid evolution of SARS-CoV-2 mandates a better understanding of cross-protection  
22 between variants after vaccination or infection, but studies directly evaluating such cross-  
23 protection are lacking. Here we report that immunization with different variant spikes elicits  
24 distinct neutralizing kinetics and magnitudes against other SARS-CoV-2 variants. After  
25 immunizing hamsters with wild-type or mutant SARS-CoV-2 bearing variant spikes from Alpha,  
26 Beta, Gamma, or Epsilon, the animals developed faster and greater neutralization activities  
27 against homologous SARS-CoV-2 variants than heterologous variants, including Delta. The  
28 rank of neutralizing titers against different heterologous variants varied, depending on the  
29 immunized variant spikes. The differences in neutralizing titers between homologous and

30 heterologous variants were as large as 62-, 15-, and 9.7-fold at days 14, 28, and 45 post-  
31 immunization, respectively. Nevertheless, all immunized hamsters were protected from  
32 challenges with all SARS-CoV-2 variants, including those exhibiting the lowest neutralizing  
33 antibody titers. The results provide insights into the COVID-19 vaccine booster strategies.

34

## 35 **Introduction**

36 The global pandemic of severe acute respiratory syndrome coronavirus 2 (SARS-CoV-2)  
37 has caused >213 million infections and >4.4 million deaths (as of August 25, 2021 per  
38 <https://coronavirus.jhu.edu/>). Despite the unprecedented success of vaccine development for  
39 coronavirus disease 2019 (COVID-19),<sup>1</sup> global control of the pandemic remains challenging  
40 because of insufficient vaccine production and vaccine hesitancy, as well as the emergence of  
41 new, more transmissible variants. Although coronaviruses have an intrinsic proofreading  
42 mechanism to maintain their long RNA genomes,<sup>2</sup> SARS-CoV-2 continues to evolve, leading to  
43 the emergence of variants. Since viral spike protein is responsible for binding to the cellular  
44 receptor angiotensin-converting enzyme 2 (ACE2), SARS-CoV-2 variants have accumulated  
45 many of their mutations in the spike gene. Such spike mutations can alter transmission  
46 efficiency and/or immune escape. The first prevalent substitution that underwent a selective  
47 sweep, D614G, is located at the spike protein that enhances spike/ACE2 binding, making the  
48 virus more transmissible.<sup>3-7</sup> Other substitutions, such as L452R and E484K in the spike  
49 receptor-binding domain (RBD), confer resistance of SARS-CoV-2 variants to therapeutic  
50 antibodies.<sup>8,9</sup> Among the emerged variants, Beta (B.1.351) and Kappa (B.1.617.1) exhibit the  
51 least sensitivity to neutralization by immune sera from vaccinated people,<sup>8,10-13</sup> whereas Alpha  
52 (B.1.1.7) and Delta (B.1.617.2) were associated with increased viral transmissibility.<sup>14,15</sup> These  
53 observations have prompted the desire to modify the vaccine sequence to match variants of  
54 concern, such as Beta because of its reduced neutralization sensitivity to the current vaccine

55 sera.<sup>8,10</sup> However, one critical question about this modified vaccine approach is whether the new  
56 vaccine elicits potent neutralizing activities against other co-circulating variants. Along the same  
57 line, cross-protection among different variants after natural infection remains to be studied in  
58 unvaccinated populations.

59

## 60 **Results**

61 To examine cross-protection among different variant spikes, we prepared a panel of four  
62 chimeric SARS-CoV-2 (**Extended Data Fig. 1a**), each bearing a distinct variant spike gene from  
63 Alpha (B.1.1.7), Beta (B.1.351), Gamma (P.1), or Epsilon (B.1.429) in the backbone of an early  
64 virus strain USA-WA1/2020 [isolated in January 2020 and defined as wild-type (WT)]. The four  
65 variants were selected based on their high prevalence at the onset of the project. Each variant  
66 spike contained a distinct set of mutations (**Fig. 1a**). An additional substitution E484K was  
67 added to the original Alpha variant (Alpha+E484K) as this mutation occurred in many clinical  
68 isolates.<sup>16</sup> The spike genes from all recombinant viruses were sequenced to ensure no aberrant  
69 mutations. Comparable ratios of viral RNA copies versus plaque-forming units (RNA/PFU) were  
70 found for both WT and chimeric viruses when produced and analyzed on Vero E6 cells  
71 (**Extended Data Fig. 1b**), suggesting equivalent specific infectivity of the viral stocks.

72 To analyze the immunogenicity of different variant spikes, we intranasally immunized  
73 hamsters with  $10^6$  PFU of recombinant WT or variant-spike virus (**Fig. 1b**). The immunized  
74 animals developed different degrees of weight loss in the order of Alpha+E484K-spike > Beta-  
75 spike  $\approx$  Gamma-spike > WT  $\approx$  Epsilon-spike (**Extended Data Fig. 2a**). The weight loss results  
76 were consistent with the clinical scores, with the Alpha+E484K-spike virus causing the most  
77 severe disease (**Extended Data figure 2b**). These results suggest that Alpha+E484K-spike is  
78 the most pathogenic virus in the hamster model. Sera were collected on days 14, 28, and 45

79 post-immunization and measured for neutralizing titers against homologous and heterologous  
80 variant-spike viruses, including the currently prevalent Delta-spike virus (**Extended Data Fig. 1**).  
81 To increase assay throughput, we developed a “fluorescent foci” reduction neutralization test  
82 (FFRNT) by using mNeonGreen (mNG) reporter viruses (**Extended Data Fig. 3a**). The mNG  
83 gene was engineered into the open-reading-frame-7 (ORF7) of the viral genome.<sup>17</sup> The  
84 protocols for the conventional plaque reduction neutralization test (PRNT) and FFRNT  
85 (**Extended Data Fig. 3b**) were similar except that the latter quantifies “fluorescent Foci” using a  
86 high-content imager in a high-throughput manner (**Extended Data Fig. 3c**). The two assays  
87 yielded comparable neutralizing titers for the same set of BNT162b2-vaccinated human sera  
88 (**Extended Data Fig. 3d,e**), validating the utility of FFRNT for neutralization test.

89 FFRNT analysis of immunized hamster sera showed distinct neutralizing profiles against  
90 homologous and heterologous SARS-CoV-2 variants (Summary in **Fig. 1c** and details in  
91 **Extended Data Fig. 4** and **Extended Data Tables 1-3**). (i) Each variant spike elicited faster and  
92 higher neutralizing titers against its homologous SARS-CoV-2 variant than heterologous  
93 variants; (ii) The magnitudes and ranks of neutralizing titers against different heterologous  
94 variants varied depending on the immunized variant spikes; (iii) Unlike other variant spike-  
95 immunized groups, the Alpha-spike-immunized animals did not seem to increase the  
96 neutralizing titers against heterologous variants from days 14 to 45 post-immunization. It is  
97 notable that from days 14 to 45 post-immunization, homologous neutralization titers increased  
98 by  $\leq 2.32$ -fold, whereas heterologous neutralization titers could increase up to 22-fold when  
99 Gamma-spike-immunized sera were tested against epsilon-spike SARS-CoV-2 (**Fig. 1c**). On  
100 days 14, 28, and 45 post-immunization, the differences in neutralizing titers between  
101 homologous and heterologous variants could be as large as 62-, 15-, 9.7-fold, respectively (**Fig.**  
102 **1c**). Collectively, the results demonstrate that vaccination of hamsters with different variant

103 spikes elicits distinct kinetics, magnitudes, and ranks of neutralizing titers against homologous  
104 and heterologous SARS-CoV-2 variants.

105 To directly evaluate cross-protection, we selected variant viruses exhibiting the lowest  
106 neutralizing titers for each immunized group to challenge the hamsters on day 49 post-  
107 immunization. Specifically, animals immunized with WT, Alpha-, Beta-, Gamma-, or Epsilon-  
108 spike were challenged with  $10^4$  PFU of Beta-, Delta-, Epsilon-, Epsilon-, and Gamma-spike  
109 SARS-CoV-2, respectively. Compared with PBS-immunized, challenged animals, all variant  
110 spike-immunized hamsters were protected from the challenge and developed significantly lower  
111 viral loads in nasal washes (82- to 10,112-fold), tracheas (955- to 120,000-fold), and lungs  
112 (57,000- to 490,000-fold) (**Fig. 1d**).

113

## 114 **Discussion**

115 Our study provided experimental evidence against the need to modify vaccine  
116 sequences to match the currently circulating SARS-CoV-2 variants of concern. Our results  
117 showed distinct cross-neutralizing profiles elicited by different variant spikes, underscoring the  
118 heterogeneity in neutralization titers against different variants for any modified spike vaccines.  
119 Such modified vaccines may pose logistic challenges for vaccine implementation because (i)  
120 multiple variants often cocirculate and (ii) the constellation of variants may differ at different  
121 geographic regions and change rapidly over time, such as the recent replacement of the Alpha  
122 by the Delta variant in many regions; these replacements have generally not been predictable.  
123 Although different vaccine choices should be prescribed depending on the prevalence of  
124 specific variants, the prescribed vaccine should also be effective against other co-circulating  
125 variants. Our results, together with the observation that BNT612b2-immunized sera remained  
126 active in neutralizing all tested variants,<sup>10-12</sup> support the strategy to continue the currently

127 approved BNT612b2 vaccine for global immunization. This strategy is further bolstered by the  
128 real-world effectiveness of two BNT612b2 doses at efficacy rates of 89.5%, 75%, and 88%  
129 against Alpha, Beta, and Delta variants, respectively<sup>18,19</sup>. When protective immunity wanes over  
130 time, a third BNT612b2 booster could be administered to enhance the overall neutralizing titers  
131 to prevent infection and disease due to new variants. However, this strategy is contingent on the  
132 sensitivity of future variants to the immunity elicited by the current vaccine. As herd immunity  
133 continues to increase through natural infection and vaccination, selective pressures for the  
134 evasion of immunity may rise. The long-term strategy should include (i) surveillance of immune  
135 escape of new variants and (ii) preparedness for changes to vaccine strains with immune  
136 escape capability.

137 A limitation of this study is the use of chimeric viruses rather than the use of clinically  
138 approved vaccine platforms for expressing variant spikes or clinical variant isolates for the  
139 challenge. The neutralizing profile elicited by chimeric viruses may differ from that elicited by the  
140 clinically approved vaccine platforms. In chimeric virus-immunized hamsters, immune  
141 responses to non-spike viral proteins may provide added protection when compared with  
142 animals immunized with spike-alone vaccines such as mRNA and adenovirus-expression  
143 platforms. Despite this limitation, it is conceivable that the relative rank of neutralizing levels  
144 would be preserved against different SARS-CoV-2 variants.

145 In summary, increasing global immunization with the currently available safe and  
146 effective vaccines, together with boosters when needed, is the strategy to end the COVID-19  
147 pandemic. The design of the booster vaccines depends on whether the newly emerged variants  
148 can escape the immunity generated by the current vaccines or natural infections. Potential  
149 immune escape of any new variants should be closely monitored by laboratory studies and real-  
150 world breakthroughs in vaccinated and infected individuals.

151

## 152 References

- 153 1 Walsh, E. E. *et al.* Safety and Immunogenicity of Two RNA-Based Covid-19 Vaccine Candidates. *N*  
154 *Engl J Med* **383**, 2439-2450, doi:10.1056/NEJMoa2027906 (2020).
- 155 2 Smith, E. C., Blanc, H., Surdel, M. C., Vignuzzi, M. & Denison, M. R. Coronaviruses lacking  
156 exoribonuclease activity are susceptible to lethal mutagenesis: evidence for proofreading and  
157 potential therapeutics. *PLoS Pathog* **9**, e1003565, doi:10.1371/journal.ppat.1003565 (2013).
- 158 3 Korber, B. *et al.* Tracking Changes in SARS-CoV-2 Spike: Evidence that D614G Increases  
159 Infectivity of the COVID-19 Virus. *Cell*, doi:10.1016/j.cell.2020.06.043 (2020).
- 160 4 Yurkovetskiy, L. *et al.* Structural and Functional Analysis of the D614G SARS-CoV-2 Spike Protein  
161 Variant. *Cell* **183**, 739-751, doi:10.1016/j.cell.2020.09.032 (2020).
- 162 5 Plante, J. A. *et al.* Spike mutation D614G alters SARS-CoV-2 fitness. *Nature* **592**, 116-121,  
163 doi:10.1038/s41586-020-2895-3 (2021).
- 164 6 Hou, Y. J. *et al.* SARS-CoV-2 D614G variant exhibits efficient replication ex vivo and transmission  
165 in vivo. *Science*, doi:10.1126/science.abe8499 (2020).
- 166 7 Zhou, B. *et al.* SARS-CoV-2 spike D614G change enhances replication and transmission. *Nature*  
167 **592**, 122-127, doi:10.1038/s41586-021-03361-1 (2021).
- 168 8 Chen, R. E. *et al.* Resistance of SARS-CoV-2 variants to neutralization by monoclonal and serum-  
169 derived polyclonal antibodies. *Nat Med* **27**, 717-726, doi:10.1038/s41591-021-01294-w (2021).
- 170 9 Xie, X. *et al.* Neutralization of SARS-CoV-2 spike 69/70 deletion, E484K and N501Y variants by  
171 BNT162b2 vaccine-elicited sera. *Nat Med* **27**, 620-621, doi:10.1038/s41591-021-01270-4 (2021).
- 172 10 Liu, Y. *et al.* Neutralizing Activity of BNT162b2-Elicited Serum. *N Engl J Med* **384**, 1466-1468,  
173 doi:10.1056/NEJMc2102017 (2021).
- 174 11 Liu, Y. *et al.* BNT162b2-Elicited Neutralization against New SARS-CoV-2 Spike Variants. *N Engl J*  
175 *Med*, doi:10.1056/NEJMc2106083 (2021).
- 176 12 Liu, J. *et al.* BNT162b2-elicited neutralization of B.1.617 and other SARS-CoV-2 variants. *Nature*,  
177 doi:10.1038/s41586-021-03693-y (2021).
- 178 13 Edara, V. V. *et al.* Infection and Vaccine-Induced Neutralizing-Antibody Responses to the SARS-  
179 CoV-2 B.1.617 Variants. *N Engl J Med*, doi:10.1056/NEJMc2107799 (2021).
- 180 14 Liu, Y. *et al.* The N501Y spike substitution enhances SARS-CoV-2 transmission. *bioRxiv*,  
181 doi:10.1101/2021.03.08.434499 (2021).
- 182 15 Hanada, K., Suzuki, Y. & Gojobori, T. A large variation in the rates of synonymous substitution for  
183 RNA viruses and its relationship to a diversity of viral infection and transmission modes. *Mol Biol*  
184 *Evol* **21**, 1074-1080, doi:10.1093/molbev/msh109 (2004).
- 185 16 Moustafa, A. M. *et al.* Comparative Analysis of Emerging B.1.1.7+E484K SARS-CoV-2 Isolates.  
186 *Open Forum Infect Dis* **8**, ofab300, doi:10.1093/ofid/ofab300 (2021).
- 187 17 Xie, X. *et al.* An Infectious cDNA Clone of SARS-CoV-2. *Cell Host Microbe* **27**, 841-848 e843,  
188 doi:10.1016/j.chom.2020.04.004 (2020).
- 189 18 Abu-Raddad, L. J., Chemaitelly, H., Butt, A. A. & National Study Group for, C.-V. Effectiveness of  
190 the BNT162b2 Covid-19 Vaccine against the B.1.1.7 and B.1.351 Variants. *N Engl J Med* **385**, 187-  
191 189, doi:10.1056/NEJMc2104974 (2021).
- 192 19 Lopez Bernal, J. *et al.* Effectiveness of Covid-19 Vaccines against the B.1.617.2 (Delta) Variant. *N*  
193 *Engl J Med* **385**, 585-594, doi:10.1056/NEJMoa2108891 (2021).
- 194 20 Xie, X. *et al.* Engineering SARS-CoV-2 using a reverse genetic system. *Nature Protocols* **16**, 1761-  
195 1784, doi:10.1038/s41596-021-00491-8 (2021).
- 196 21 Muruato, A. E. *et al.* A high-throughput neutralizing antibody assay for COVID-19 diagnosis and  
197 vaccine evaluation. *Nature Communications* **11**, 4059, doi:10.1038/s41467-020-17892-0 (2020).

198



199 **Methods**

200 **Ethics statement.** Hamster studies were performed under the guidance of the Care and  
201 Use of Laboratory Animals of the University of Texas Medical Branch (UTMB). The protocol was  
202 approved by the Institutional Animal Care and Use Committee (IACUC) at UTMB. All the  
203 hamster operations were performed under anesthesia by isoflurane to minimize animal suffering.

204 **Animals and Cells.** The Syrian golden hamsters (HsdHan:AURA strain) were purchased  
205 from Envigo (Indianapolis, IN). Vero E6 cells, an African green monkey kidney epithelial cell line  
206 (ATCC, Manassas, VA, USA), were cultured in Dulbecco's modified Eagle's medium (DMEM;  
207 Gibco/Thermo Fisher, Waltham, MA, USA) with 10% fetal bovine serum (FBS; HyClone  
208 Laboratories, South Logan, UT) plus 1% ampicillin/streptomycin (Gibco). The authenticity of  
209 Vero E6 cells was verified using Short Tandem Repeat profiling by ATCC. The cells were tested  
210 negative for mycoplasma.

211 **Construction of chimeric SARS-CoV-2s with variant spikes and mNeonGreen**  
212 **(mNG) reporter viruses.** All spike mutations from different variants were engineered into an  
213 infectious cDNA clone of an early SARS-CoV-2 isolate USA-WA1/2020 using a standard PCR-  
214 based mutagenesis method. The protocol for the construction of recombinant SARS-CoV-2 was  
215 reported previously.<sup>17,20</sup> To construct the mNG reporter viruses with variant spikes, the mNG  
216 gene was engineered into the open-reading-frame-7 (ORF7) of the viral genome. The full-length  
217 cDNAs of the viral genome containing the variant spike mutations were assembled by in vitro  
218 ligation. The resulting genome-length cDNAs served as templates for in vitro transcription of full-  
219 length viral RNAs. The full-length viral RNA transcripts were electroporated into Vero E6 cells.  
220 On day 2 post electroporation (when the electroporated cells developed cytopathic effects due  
221 to recombinant virus production and replication), the original viral stocks (P0) were harvested  
222 from the culture medium. The P0 viruses were amplified on Vero E6 cells for another round to

223 produce working viral stocks (P1). The complete spike genes from the P1 viruses were  
224 sequenced to ensure no undesired mutations. The P1 viruses were used for the following study.

225 **Plaque assay.** Approximately  $1.2 \times 10^6$  Vero E6 cells were seeded to each well of 6-well  
226 plates and cultured at 37°C, 5% CO<sub>2</sub> for 16 h. The virus was serially diluted in DMEM with 2%  
227 FBS and 200 µl diluted viruses were transferred onto the monolayer of Vero E6 cells. The  
228 viruses were incubated with the cells at 37°C with 5% CO<sub>2</sub> for 1 h. After the incubation, 2 ml of  
229 overlay medium (DMEM medium supplemented with 1% agar) was added to the infected cells  
230 per well. The overlay medium contained DMEM with 2% FBS, 1% penicillin/streptomycin, and 1%  
231 sea-plaque agarose (Lonza, Walkersville, MD). After a 2-day incubation, plates were stained  
232 with neutral red (Sigma-Aldrich, St. Louis, MO) and plaques were counted on a lightbox.

233 **Quantitative real-time RT-PCR assays.** RNA copies of SARS-CoV-2 samples were  
234 detected by quantitative real-time RT-PCR (RT-qPCR) assays were performed using the iTaq  
235 SYBR Green One-Step Kit (Bio-Rad) on the LightCycler 480 system (Roche, Indianapolis, IN)  
236 following the manufacturer's protocols. The absolute quantification of viral RNA was determined  
237 by a standard curve method using an RNA standard (*in vitro* transcribed 3,480 bp containing  
238 genomic nucleotide positions 26,044 to 29,883 of SARS-CoV-2 genome).

239 **Hamster infections.** Four- to six-week-old male golden Syrian hamsters, strain  
240 HsdHan:AURA (Envigo, Indianapolis, IN), were intranasally immunized with  $10^6$  PFU  
241 recombinant WT or variant spike virus on day 0. The immunized animals were weighed and  
242 monitored for signs of illness daily. Sera were collected on days 14, 28, and 45 post-  
243 immunization and measured for neutralizing titers against homologous and heterologous  
244 variant-spike viruses. On day 49, animals from each immunized group were challenged with  $10^4$   
245 PFU of selected variant viruses exhibiting the lowest neutralizing titers. Specifically, animals  
246 immunized with WT, Alpha-, Beta-, Gamma-, or Epsilon-spike were challenged with the Beta-,  
247 Delta-, Epsilon-, Epsilon-, and Gamma-spike SARS-CoV-2, respectively. Nasal washes were

248 collected in 400 µl sterile DPBS at indicated time points. Animals were humanely euthanized for  
249 organ collections after 2 days of the challenge. The harvested tracheae and lungs were placed  
250 in a 2-ml homogenizer tube containing 1 ml of maintenance media (DMEM supplemented with 2%  
251 FBS and 1% penicillin/streptomycin) and stored at -80°C. Samples were subsequently thawed,  
252 lung or tracheae were homogenized using TissueLyser II (Qiagen, Hilden, Germany) for 1 min  
253 at 26 sec<sup>-1</sup>, and debris was pelleted by centrifugation for 5 min at 16,100×g. Infectious titers  
254 were determined by plaque assay.

255 **Human serum specimens.** The research protocol regarding the use of human serum  
256 specimens was reviewed and approved by the University of Texas Medical Branch (UTMB)  
257 Institutional Review Board. The approved IRB protocol number is 20-0070. All human serum  
258 specimens were obtained from the vaccinated subjects at the UTMB. All specimens were de-  
259 identified from patient information.

260 **Fluorescent foci reduction neutralization assay.** Neutralization titers of human and  
261 hamster sera were measured by fluorescent foci reduction neutralization assay (FFRNT) using  
262 the mNG SARS-CoV-2. Briefly, Vero E6 cells ( $2.5 \times 10^4$ ) were seeded in each well of black  
263 CLEAR flat-bottom 96-well plate (Greiner Bio-one™). The cells were incubated overnight at  
264 37°C with 5% CO<sub>2</sub>. On the following day, each serum was 2-fold serially diluted in the culture  
265 medium with the first dilution of 1:10. The diluted serum was incubated with 100 PFU of mNG  
266 SARS-CoV-2 at 37 °C for 1 h (final dilution range of 1:20 to 1:5120), after which the serum-virus  
267 mixtures were inoculated onto Vero E6 cell monolayer in 96-well plates. After 1 h of infection,  
268 the inoculum was removed and 100 µl of overlay medium (DMEM supplemented with 0.8%  
269 methylcellulose, 2% FBS, and 1% P/S) was added to each well. The plates were incubated at  
270 37°C for 20 h. The raw images were acquired using Cytation™ 7 (BioTek) armed with 2.5×  
271 objective and processed using the default software setting. The foci in each well were counted  
272 and normalized to the non-serum-treated controls to calculate the relative infectivities. The

273 curves of the relative infectivity versus the serum dilutions (log<sub>10</sub> values) were plotted using  
274 Prism 9 (GraphPad). A nonlinear regression method was used to determine the dilution fold that  
275 neutralized 50% of mNG SARS-CoV-2 (defined as FFRNT). Each serum was tested in  
276 duplicates.

277 **Plaque reduction neutralization test (PRNT).** A conventional 50% plaque-reduction  
278 neutralization test (PRNT<sub>50</sub>) was performed to measure the serum-mediated virus suppression  
279 as reported previously<sup>21</sup>. Individual sera were 2-fold serially diluted in culture medium with a  
280 starting dilution of 1:40 (dilution range of 1:40 to 1:1280). The diluted sera were incubated with  
281 100 PFU of USA-WA1/2020 (WT) or mutant SARS-CoV-2. After 1 h incubation at 37°C, the  
282 serum-virus mixtures were inoculated onto 6-well plates with a monolayer of Vero E6 cells pre-  
283 seeded on the previous day. The minimal serum dilution that suppressed >50% of viral plaques  
284 is defined as PRNT<sub>50</sub>.

285

## 286 **Data availability**

287 The data that support the findings of this study are available from the corresponding  
288 authors upon reasonable request.

289

## 290 **Acknowledgments**

291 We thank Phillip R. Dormitzer for his helpful discussions during the study. P.-Y.S. was  
292 supported by NIH grants HHSN272201600013C, AI134907, AI145617, and UL1TR001439, and  
293 awards from the Sealy & Smith Foundation, the Kleberg Foundation, the John S. Dunn  
294 Foundation, the Amon G. Carter Foundation, the Gilson Longenbaugh Foundation, and the  
295 Summerfield Robert Foundation. S.C.W. was supported by NIH grant R24 AI120942. P.R. and

296 X.X. were partially supported by the Sealy & Smith Foundation. J.L. was supported by James W.  
297 McLaughlin Fellowship Fund.

298

### 299 **Author contributions**

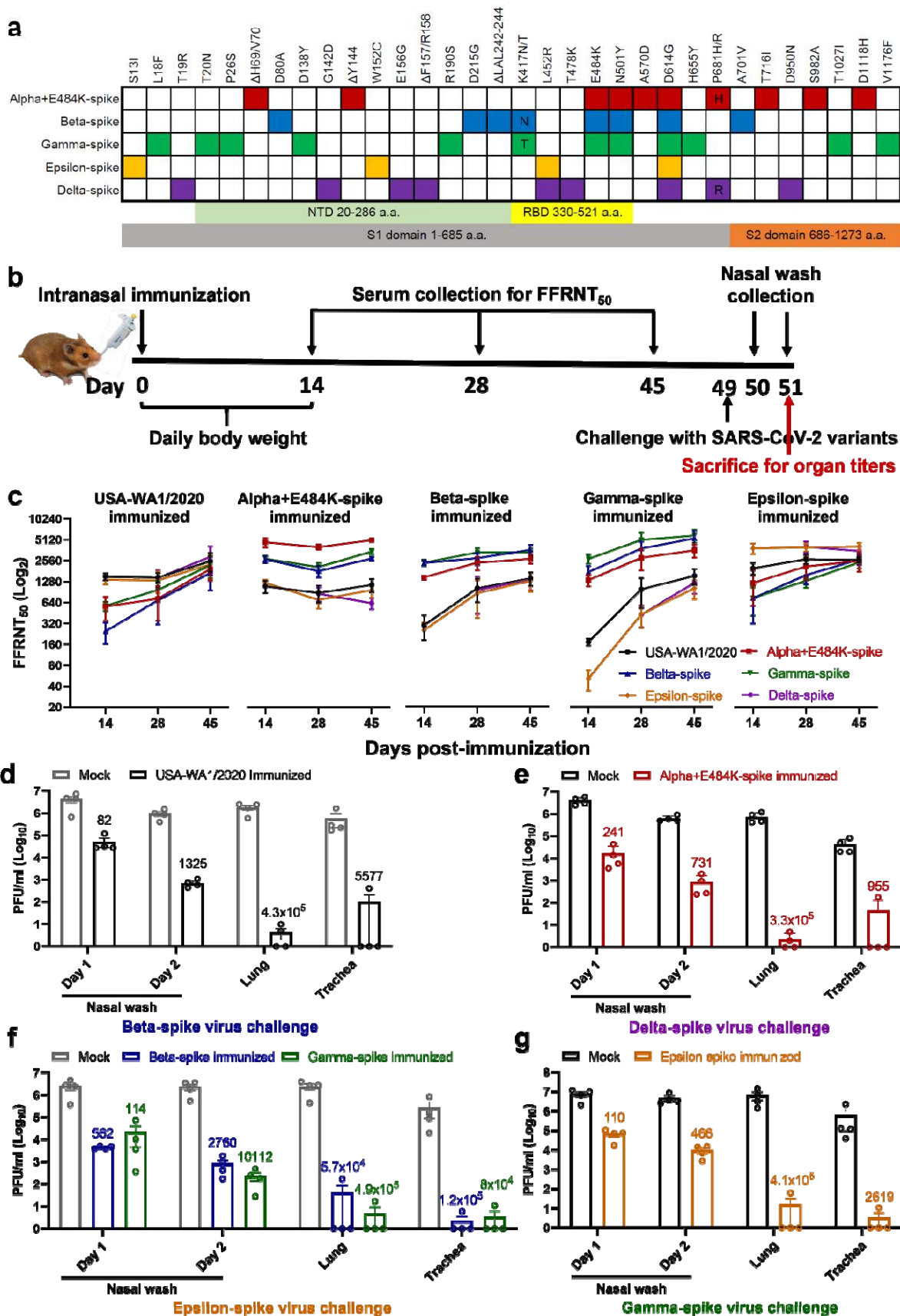
300 Conceptualization, Y.L., S.C.W., X.X., P.-Y.S.; Methodology, Y.L. J.L., J.Z., X.X., P.-Y.S;  
301 Investigation, Y.L., J.L., J.Z., S.C.W., X.X., P.-Y.S.; Resources, P.R., S.C.W., P.-Y.S.; Data  
302 Curation, Y.L., J.L., J.Z., X.X., P.-Y.S.; Writing-Original Draft, Y.L., X.X., P.-Y.S.; Writing-Review  
303 & Editing, Y.L., J.L., J.Z., P.R., S.C.W., X.X., P.-Y.S.; Supervision, S.C.W., X.X., P.-Y.S.;  
304 Funding Acquisition P.-Y.S..

305

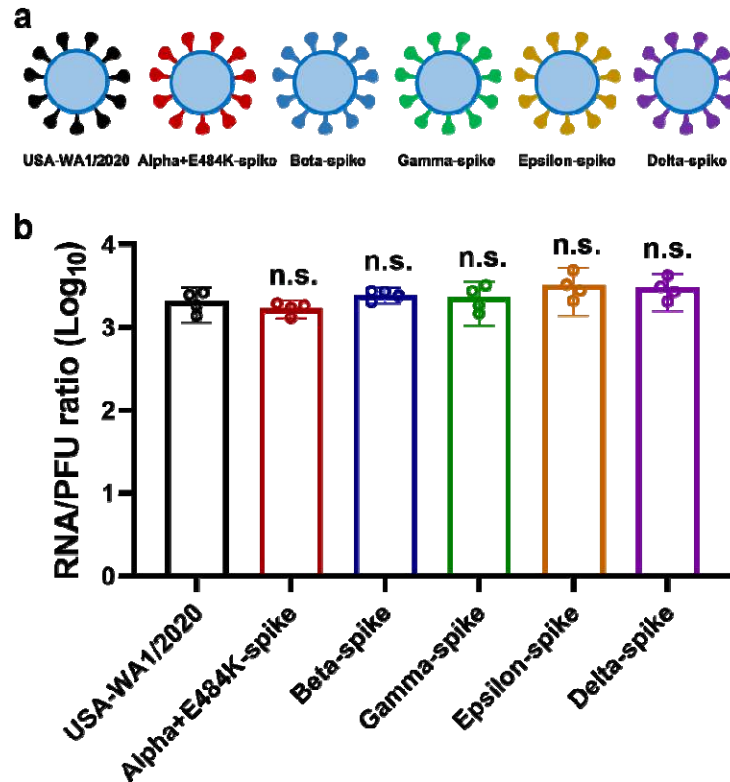
### 306 **Competing financial interests**

307 X.X. and P.-Y.S. have filed a patent on the reverse genetic system. Other authors  
308 declare no competing interests.

309



311 **Figure 1. Variant spikes elicit neutralizing antibodies that cross-protect hamsters from**  
312 **challenges with SARS-CoV-2 variants. a,** Amino acid substitutions in the spike protein among  
313 SARS-CoV-2 variants. The sequence of the spike from USA-WA1/2020 strain was used as a  
314 reference. NTD, N-terminal domain; RBD, Receptor binding domain. **b,** Experimental scheme of  
315 immunization and challenge in hamsters. The hamsters (n=4 per group) were intranasally  
316 immunized with  $10^6$  PFU of WT or variant-spike SARS-CoV-2. Serum specimens were  
317 measured for FFRNT<sub>50</sub> values on days 14, 28, and 45 post-immunization. On day 49 post-  
318 immunization, the hamsters were intranasally challenged by the indicated variant-spike SARS-  
319 CoV-2 ( $10^4$  PFU). The nasal washes were quantified for viral titers on days 1 and 2 post-  
320 challenge. All the hamsters were sacrificed on day 2 post-challenge for viral titers detection. **c,**  
321 Neutralization titers of hamster sera against SARS-CoV-2 spike variants on days 14, 28, and 45  
322 post-immunization. Means  $\pm$  standard errors of the mean are shown. **d-g,** Protection of  
323 immunized hamsters from the challenge of SARS-CoV-2 spike variants. The immunized  
324 hamsters and age-matched non-immunized hamsters (Mock) were challenged with selected  
325 variant viruses exhibiting the lowest neutralizing titers. The viral loads in the nasal wash (NW,  
326 days 1 and 2), lung, and trachea (day 2) were detected by plaque assays. The numbers above  
327 individual columns indicate the fold decrease in viral loads by comparing the means from the  
328 immunized group with that from the non-immunized mock group. Means  $\pm$  standard errors of the  
329 mean are shown. The assay limit is 10 PFU/ml.



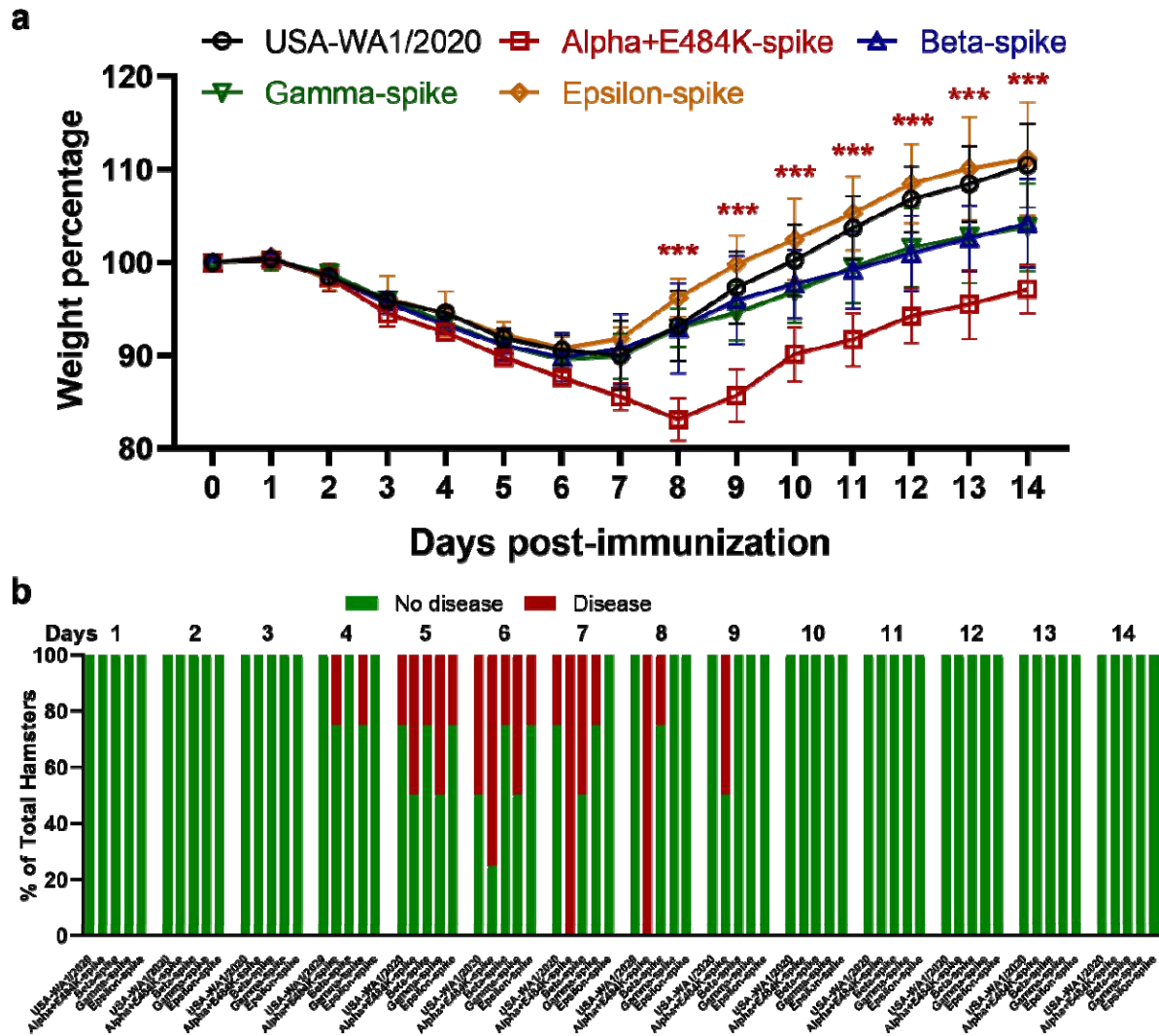
330

331

332 **Extended Data Figure 1. The RNA/PFU ratios of different SARS-CoV-2 variants.**

333 **a**, Diagram of SARS-CoV-2 spike variants. The spike genes from Alpha, Beta, Gamma, Epsilon,  
334 and Delta variants of SARS-CoV-2 were introduced into USA-WA1/2020 backbone. **b**, Ratios of  
335 viral genomic RNA versus plaque-forming unit (RNA/PFU) of SARS-CoV-2 spike variants. The  
336 genomic RNA and PFU of individual viral stocks were measured by RT-qPCR and plaque assay,  
337 respectively. The USA-WA1/2020 strain served as a control. Dots represent individual biological  
338 replicates from 4 aliquots of viruses. The means with 95% confidence intervals are shown. A  
339 non-parametric Mann-Whitney test was used to determine significant differences between USA-  
340 WA1/2020 and other variants.  $P$  values were adjusted using the Bonferroni correction to  
341 account for multiple comparisons. Differences were considered significant if  $P < 0.05$ ; n.s., no  
342 statistical difference.

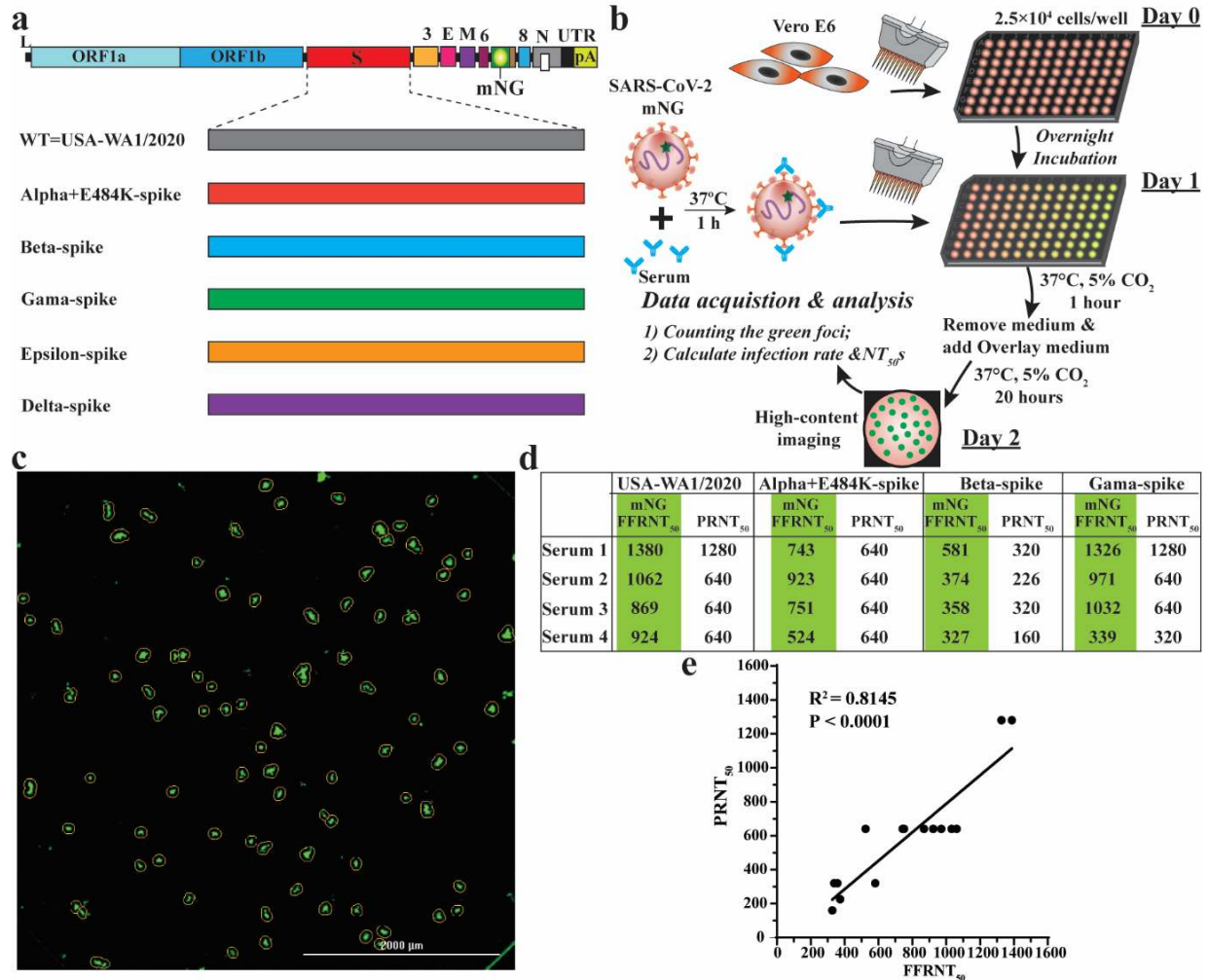




343

344 **Extended Data Figure 2. Morbidity of hamsters after immunized with variant-spike SARS-**  
 345 **CoV-2.**

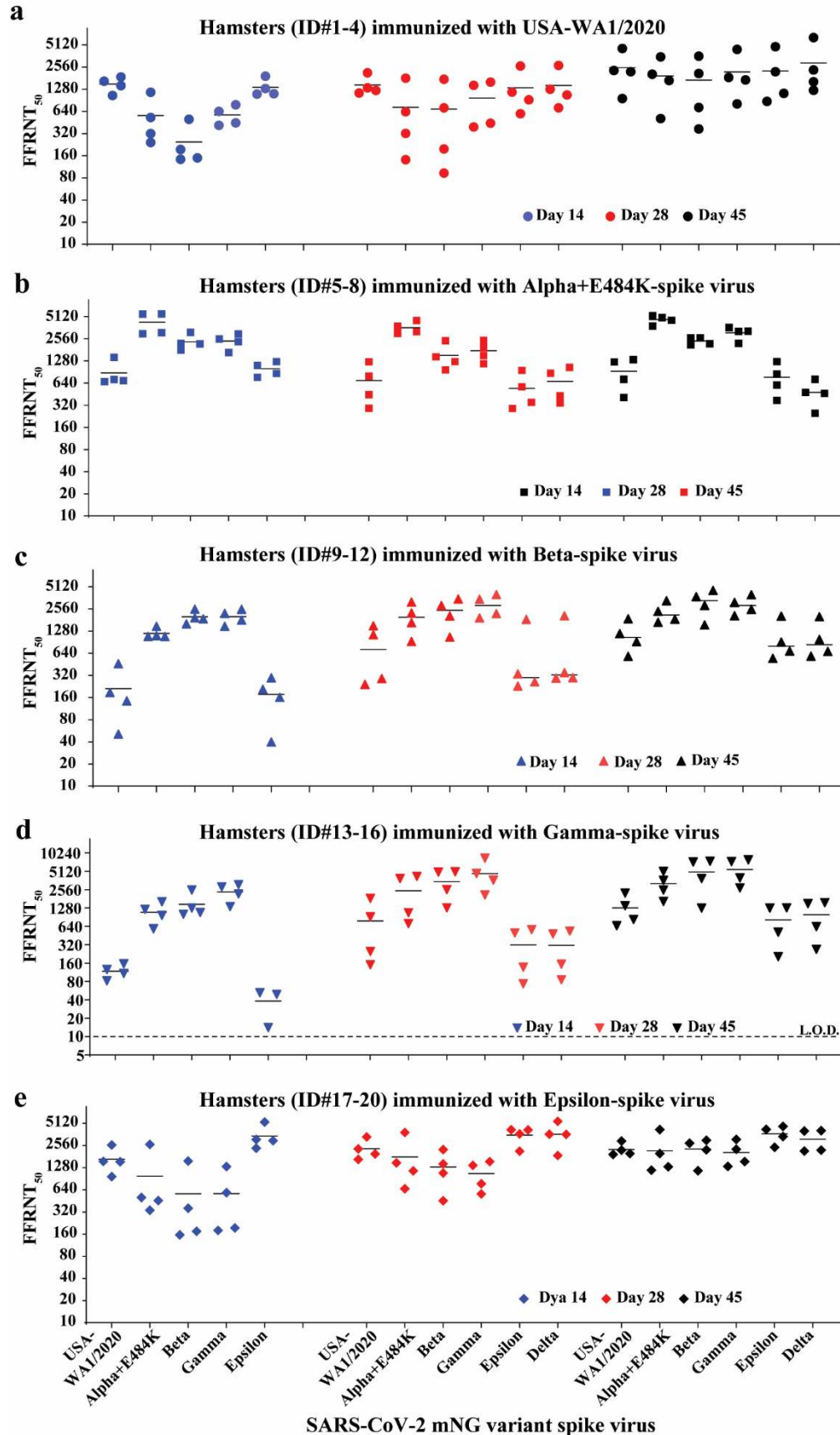
346 **a**, Hamster body weight loss after immunized with variant-spike SARS-CoV-2. The hamsters  
 347 (n=4) were intranasally infected with  $10^6$  PFU viruses. The body weights were measured daily  
 348 from day 0 to day 14 days post-immunization. The weight loss data are shown as mean  $\pm$   
 349 standard deviation and statistically analyzed using two-way ANOVA Turkey's multiple  
 350 comparisons. The red stars show the statistical significance (\*\*\*)  $P < 0.001$ ) between USA-  
 351 WA1/2020-immunized hamsters and Alpha+E484K-spike-immunized hamsters. **b**, Percentages  
 352 of hamsters with or without diseases (including ruffled fur, lethargic, hunched, and reluctance to  
 353 move when stimulated) from day 1 to day 14 post-immunization.



354

355 **Extended Data Figure 3. Correlation between FFRNT<sub>50</sub> and PRNT<sub>50</sub>.**

356 **a**, Diagram of mNG USA-WA1/2020 and spike variants. mNG, mNeogreen fluorescence  
 357 protein gene. **b**, Workflow of fluorescent foci reduction neutralization (FFRNT) assay. The  
 358 details of the FFRNT assay were described in the Methods. **c**, Representative images of foci  
 359 formed in a 96-well plate after 20 h of infection. **d**, FFRNT<sub>50</sub> and PRNT<sub>50</sub> values for four human  
 360 sera. The FFRNT<sub>50</sub> values are shaded in green. **e**, Correlation of FFRNT<sub>50</sub> and PRNT<sub>50</sub>. The  
 361 Pearson's correlation coefficients and *P* values (two-tailed) are indicated.



363 **Extended Data Figure 4. FFRNT<sub>50</sub>s of hamster sera against mNG SARS-CoV-2 spike**  
364 **variants on days 14, 28, and 45 post-immunization.**  
365 **a-e**, Hamster (n=4 per group) were immunized with WT USA-WA1/2020 (**a**), Alpha+E484K-  
366 spike virus (**b**), Beta-spike virus (**c**), Gamma-spike virus (**d**), Epsilon-spike virus (**e**). Sera were  
367 collected on days 14, 28, and 45 post-immunization and tested for neutralizing activities against  
368 the indicated mNG viruses by FFRNT. The original FFRNT<sub>50</sub> values are presented in **Extended**  
369 **Data Tables 1-3.**

**Extended Data Table 1. FFRNT<sub>50</sub>s of twenty hamster sera on day 14 post-immunization.**

Virus for infection	Hamster ID	FFRNT <sub>50</sub> s against SARS-CoV-2 spike variants				
		USA-WA1/2020 mNG	Alpha+E484K-spike mNG	Beta-spike mNG	Gamma-spike mNG	Epsilon-spike mNG
USA-WA1/2020	1	1048	320	194	446	1113
	2	1875	1158	498	785	1916
	3	1643	242	143	413	1304
	4	1426	528	149	637	1099
	Mean	1498	562	246	570	1358
Alpha+E484K-spike	5	689	5561	1789	1660	1111
	6	669	5526	2214	2543	864
	7	1431	2981	3122	2967	762
	8	714	3087	2175	2318	1246
	Mean	876	4289	2325	2372	996
Beta-spike	9	461	1079	1610	2226	296
	10	188	1482	2537	2520	161
	11	51	1082	1947	1486	40
	12	144	1113	1881	1802	208
	Mean	211	1189	1994	2009	176
Gamma-spike	13	108	1215	2525	2833	49
	14	125	583	1006	1346	<10
	15	155	967	1075	2166	14
	16	82	1617	1275	3092	52
	Mean	118	1096	1470	2359	38
Epsilon-spike	17	966	337	156	194	2346
	18	2602	502	358	583	5297
	19	1535	457	175	179	2977
	20	1552	2637	1572	1321	3085
	Mean	1664	983	565	569	3426

**Extended Data Table 2. FFRNT<sub>50</sub>s of twenty hamster sera on day 28 post-immunization.**

Virus for infection	Hamster ID	FFRNT <sub>50</sub> s against SARS-CoV-2 spike variants					
		USA-WA1/2020 mNG	Alpha+E484K-spike mNG	Beta-spike mNG	Gamma-spike mNG	Epsilon-spike mNG	Delta-spike mNG
USA-WA1/2020	1	1226	632	714	1601	1167	1278
	2	2140	1807	1749	1442	2646	2691
	3	1137	141	93	392	920	713
	4	1336	321	197	442	594	1068
	Mean	1460	725	688	969	1332	1438
Alpha+E484K-spike	5	445	3007	963	1169	288	430
	6	1239	4511	1453	1920	950	1044
	7	792	3174	1248	1507	569	867
	8	291	3787	2405	2425	349	343
	Mean	692	3620	1517	1755	539	671
Beta-spike	9	1511	3184	3494	4027	1850	2068
	10	241	1671	2048	2209	230	293
	11	1144	2253	2848	3473	336	349
	12	290	931	1059	1932	261	299
	Mean	797	2010	2362	2910	669	752
Gamma-spike	13	914	3874	5009	4685	564	480
	14	1837	4197	4954	8391	498	535
	15	247	707	1282	2090	73	85
	16	150	1068	2555	3644	137	153
	Mean	787	2462	3450	4703	318	313
Epsilon-spike	17	1961	1484	1080	770	3683	5442
	18	3347	1153	1432	1373	4163	3634
	19	1654	662	455	562	2132	1868
	20	2298	3833	2251	1545	4182	3605
	Mean	2315	1783	1305	1063	3540	3637

**Extended Data Table 3. FFRNT<sub>50</sub>s of twenty hamster sera on day 45 post-immunization.**

Virus for infection	Hamster ID	FFRNT <sub>50</sub> s against SARS-CoV-2 spike variants					
		USA-WA1/2020	Alpha+E484K-spike	Beta-spike	Gamma-spike	Epsilon-spike	Delta-spike
		mNG	mNG	mNG	mNG	mNG	mNG
USA-WA1/2020	1	4574	3509	3590	4437	4843	6410
	2	2299	2042	2094	1850	2207	2337
	3	953	510	370	807	1125	1612
	4	2205	1682	723	1707	871	1232
	Mean	2508	1936	1694	2200	2262	2898
Alpha+E484K-spike	5	718	3794	2628	3627	601	462
	6	1326	5262	2624	3211	1248	719
	7	1237	4554	2115	3225	844	477
	8	405	4930	2181	2210	372	248
	Mean	922	4635	2387	3068	766	477
Beta-spike	9	1881	3305	4574	3994	2047	2005
	10	582	1852	2857	2527	545	584
	11	1184	2374	3746	3139	906	988
	12	920	1692	1554	2068	688	680
	Mean	1142	2306	3183	2932	1047	1064
Gamma-spike	13	1391	3638	7481	7345	1272	1505
	14	2251	5095	7255	7892	1282	1566
	15	656	1638	1274	2734	203	268
	16	828	2521	3882	3986	514	633
	Mean	1282	3223	4973	5489	818	993
Epsilon-spike	17	1982	1315	2236	1548	3379	2149
	18	2205	1991	2742	3084	4212	4069
	19	1928	1182	1158	1326	2419	2208
	20	2930	4189	3004	2268	4641	4016
	Mean	2261	2169	2285	2057	3663	3111